processes

MDPI

Article

Preparation and Phosphorus Removal Performance of Zr–La–Fe Ternary Composite Adsorbent Embedded with Sodium Alginate

Xiuling Li, Hanyu Liang, Yanling Mo and Yansong Wei *

College of Chemical and Biological Engineering, Hechi University, Yizhou 546300, China
* Correspondence: 06020@hcnu.edu.cn; Tel.: +86-13607786565

Abstract: Using single metal salts of zirconium, lanthanum, and iron as raw materials and sodium alginate as a cross-linking agent, a new composite adsorbent was prepared via the co-precipitation method and embedding immobilization technology, and its phosphorus adsorption performance in wastewater was evaluated. Scanning electron microscopy (SEM), Fourier transform infrared spectroscopy (FT-IR), X-ray diffraction (XRD), and X-ray photoelectron spectroscopy (XPS) were used for characterization, and a 0.5 mol·L^{-1} sodium hydroxide solution was used to regenerate the adsorbent. The experimental results demonstrated that the adsorption rate reached 99.88% when the wastewater volume was 50 mL, the initial concentration of phosphorus-containing wastewater was 5 mg·L^{-1}, the pH was 5, the dosage of composite adsorbent was 0.2 g, and the adsorption time was 200 min. The prepared adsorbent could reduce the initial phosphorus concentration of 5 mg·L^{-1} to 0.006 mg·L^{-1} in simulated wastewater, and from 4.17 mg·L^{-1} in urban sewage to undetected (<0.01 mg·L^{-1}), thus meeting the discharge requirements of the grade A standard of the Urban Sewage Treatment Plant Pollutant Discharge Standard (GB18918-2002). The adsorption process conformed to the Freundlich adsorption isothermal equation and quasi-second-order kinetic equation, and the adsorption reaction was exothermic and spontaneous. More importantly, after three lye regeneration tests, the removal rate of phosphorus in water remained above 68%, that is, the composite adsorbent could be reproducibly fabricated and recycled. The characterization results showed that the surface of the composite adsorbent was rough, with a complex pore structure. After phosphorus removal, the surface morphology of the composite adsorbent showed a similar honeycomb structure, with a P-H, P-O stretching vibration peak and a characteristic P2p peak. At the same time, the proportion of hydroxyl groups (M-OH) on the metal surface decreased after adsorption. Our findings thus demonstrate that the mechanism of phosphorus removal is mainly based on the coordination exchange reaction between phosphate and metal active sites and surface hydroxyl groups, resulting in the formation of granular phosphate deposits.

Keywords: sodium alginate; Zr–La–Fe; composite adsorbent; phosphorus removal; regeneration

Citation: Li, X.; Liang, H.; Mo, Y.; Wei, Y. Preparation and Phosphorus Removal Performance of Zr–La–Fe Ternary Composite Adsorbent Embedded with Sodium Alginate. *Processes* **2022**, *10*, 1761. https://doi.org/10.3390/pr10091761

Academic Editors: Dimitris Zagklis and Georgios Bampos

Received: 29 July 2022
Accepted: 29 August 2022
Published: 2 September 2022

1. Introduction

Due to the increase in industrial output and human activities, such as the excessive use of phosphorus fertilizer and pesticides in rural areas, and the arbitrary discharge of livestock and poultry breeding wastewater, large amounts of phosphorus are discharged into aquatic environments and cause eutrophication, which leads to water hypoxia, a large amount death to aquatic life, human gastrointestinal disease, and so on. Urban sewage treatment plants are responsible for treating sewage water. However, urban sewage treatment plants must be urgently upgraded to further improve sewage treatment capacity and treatment standards, meet the requirements of China's key river basin environmental governance, and alleviate water eutrophication. This would facilitate compliance with the "Urban Sewage Treatment Plant Pollutant Discharge Standard" (GB18918-2002), in addition to reducing phosphorus discharge through in-depth treatment. Therefore, research on phosphorus removal from wastewater has recently garnered increasing attention.

Current phosphorus removal methods include chemical precipitation [1–3], biological methods [4–6], and adsorption [7–10]. Among these, adsorption can be easily and stably implemented and delivers good effluent quality [11]. This approach can not only be used to supplement biological phosphorus removal for the treatment of wastewater with low phosphorus concentrations, but can also be used as a stand-alone method for the treatment of wastewater with high phosphorus concentrations. Moreover, phosphorus removal by adsorption does not cause secondary pollution, and the adsorbed phosphate can be desorbed and recovered. Therefore, the adsorption method has become a widely used treatment technology in the field of phosphorus wastewater treatment.

Studies have found that some metal elements such as Zr, Fe, La, and Mn have strong affinities for phosphorus, and single or binary composite oxides of these metal elements can be synthesized as adsorbents to remove excess phosphorus in water [12–19]. According to the existing literature, we find that lanthanum is a kind of benign rare-earth material that is rich in reserves, environmentally friendly, and non-toxic. Due to its strong binding ability to phosphate ($LaPO_4$ pKsp = 26.16), it can exhibit a strong affinity for phosphorus. Meanwhile, iron (Fe) and zirconium (Zr) compounds are widely used for phosphate removal in wastewater treatment due to their higher surface charge, lower cost, and higher resistance to acid, alkali, oxidant and reducing agent compared to La, which could stably adsorb phosphate in a wider pH range [20]. Multi-metal oxide composites usually exhibit significantly different physical and chemical properties from their single-component oxides and can combine the advantages of single metals, which improves phosphate adsorption performance to a certain extent. Thereby, we chose the single metal salts of zirconium, lanthanum, and iron as raw materials to prepare a new composite adsorbent. However, recent studies have demonstrated that ternary composite adsorbents show greater advantages in phosphorus removal from water compared to other conventionally used materials. Yu et al. [21] synthesized an Fe–Mg–La ternary metal complex for phosphorus removal in water, which reached its maximum adsorption of 415.2 $mg \cdot g^{-1}$ at a pH of 6.0. Yang et al. [22] prepared an Fe–Mg–La ternary composite adsorbent and its maximum adsorption capacity was 30.16 $mg \cdot g^{-1}$ at a pH of 3.02. Lu et al. [23] synthesized an Fe–Al–Mn ternary composite adsorbent by adding alumina to Fe–Mn to improve adsorption and phosphorus removal performance.

Although the aforementioned adsorbents can effectively remove phosphate from water, most of them occur in powder form and, therefore, cannot be easily separated and recycled. Sodium alginate is a kind of biopolymer that contains large amounts of reactive functional groups, such as -COOH and -OH. The presence of calcium ions in aqueous solution can induce the formation of a three-dimensional mesh structure of salt alginate gel particles via ion exchange-mediated polymerization. In turn, this immobilizes powdery adsorbents into a granular material, which not only improves adsorbent settlement but also facilitates its recovery and utilization. Additionally, sodium alginate is safe, stable, non-toxic, environmentally friendly, and does not cause secondary water pollution.

Therefore, based on the findings of previous studies, our study employs three metal salts of zirconium, lanthanum, and iron as raw materials, and sodium alginate was used as a crosslinking agent to prepare a new type of ternary composite adsorbent via the co-precipitation method coupled with embedding immobilization technology. The adsorption performance of the composite adsorbent on phosphorus in water was characterized by XRD, SEM, XPS, and FT-IR. Moreover, the phosphorus removal mechanism of the composite adsorbent was studied to establish a novel approach for the treatment of phosphorus-containing wastewater.

2. Experimental

2.1. Materials

$LaCl_3 \cdot 7H_2O$, $Fe(NO_3)_3 \cdot 9H_2O$, $ZrOCl_2 \cdot 8H_2O$, KH_2PO_4, H_2SO_4, HCl, NaOH, $K_2S_2O_8$, $C_6H_8O_6$, $(NH_4)_6MoO_{24} \cdot 4H_2O$, and $K(SbO)C_4H_4O_6 \cdot 5H_2O$ were purchased from Tianjin Kemi Ou Chemical Co., LTD. (Tianjin, China) All reagents were of analytical grade.

Potassium dihydrogen phosphate (KH_2PO_4) was used to prepare a phosphorus stock solution (1000 mg·L^{-1}), and simulated wastewater with different phosphorus levels was prepared by diluting this stock solution to the desired concentrations. Wastewater samples were collected from the outlet of the secondary sedimentation tank of the First Sewage Treatment Plant in Yizhou, Hechi, Guangxi.

2.2. Preparation of Zr–La–Fe Ternary Adsorbent Embedded with Sodium Alginate

Certain masses of $ZrOCl_2 \cdot 8H_2O$, $LaCl_3 \cdot 7H_2O$, and $Fe(NO_3)_3 \cdot 9H_2O$ were weighed, dissolved and shaken in 250 mL of deionized water, and the three dissolved materials were poured into a 1 L beaker, stirred, and shaken. The pH value of the mixture was then adjusted to 8.00 by slowly adding a 2 mol·L^{-1} NaOH solution, and a suspension gradually appeared when adding the alkali. Next, the mixture was transferred to a blender and stirred for more than 1 hour. The finished mixture was transferred to a round-bottom flask, the temperature of the water bath thermostat was adjusted to 25 °C, and the solution was allowed to age for 24–30 h. The solution was then removed, and the solids were washed with deionized water while measuring the pH value of the solution. Once the pH was neutral, the mixture was placed in a suction filter machine for extraction and filtration, after which the adsorption material was transferred to a 70 °C oven for drying. After drying, the resulting Zr–La–Fe ternary composite material was ground and sieved.

Next, the prepared Zr–La–Fe ternary composite adsorbent was immobilized with sodium alginate. A certain amount of sodium alginate was first weighed and dissolved in water, after which the mixture was transferred to a volumetric flask. A certain proportion of sodium alginate was then added to the Zr–La–Fe terpolymer adsorbent, after which the preparation was stirred, evenly dispersed, and slowly added to an aqueous solution with a certain concentration of calcium chloride. After soaking and cross-linking, the solids were washed 2–3 times with deionized water. After drying in an oven at 85 °C, the composite adsorbent required for phosphorus removal in this experiment was obtained.

2.3. Sample Characterization

The composition and internal morphology of the composite adsorbent were analyzed by XRD. The groups and structures of the composite adsorbent were analyzed by characterizing its FT-IR spectra. The morphology features of the composite adsorbent were analyzed by SEM. The elemental composition of the composite adsorbent was analyzed based on its XPS spectra. Point-of-zero-charge measurements were conducted to evaluate the surface charge distribution of the composite adsorbent under different pH conditions.

2.4. Experimental Methods

The wastewater volume in the adsorption experiment was fixed at 50 mL, the rotating speed of the shaker was 180 r·min^{-1}, and the adsorption experiment was carried out in a 250 mL conical flask. Different experimental conditions were changed to study the influence of various factors on phosphorus removal. After adsorption, the wastewater was filtered with a 0.45 μm drainage membrane and the residual phosphorus concentration was determined by spectrophotometry. The phosphorus removal rate (E) and adsorption capacity (Q_e) were used as evaluation indices, and the calculation formula was as follows:

$$E = \frac{(C_0 - C_e)}{C_0} \times 100\% \quad (1)$$

$$Q_e = \frac{(C_0 - C_e) \cdot V}{m \times 1000} \quad (2)$$

where C_0 is the initial concentration of total phosphorus, mg·L^{-1}; C_e is the equilibrium concentration of total phosphorus, mg·L^{-1}; V is the volume of simulated wastewater containing phosphorus, mL; m is the dosage of adsorbent, g; and Q_e is the equilibrium adsorption capacity, mg·g^{-1}.

2.5. Thermodynamic and Kinetic Fitting of Adsorption

2.5.1. Thermodynamic Fitting of Adsorption

Langmuir adsorption isotherm [24]:

$$\frac{1}{Q_e} = \frac{K_L}{Q_m C_e} + \frac{1}{Q_m} \tag{3}$$

where C_e and Q_e represent the same as in Equations (1) and (2); Q_m is the maximum adsorption capacity, mg·g^{-1}; K_L is the equilibrium constant.

Freundlich sorption isotherm [25]:

$$lgQ_e = lgK_F + \frac{1}{n} lgC_e \tag{4}$$

where C_e and Q_e represent the same as in Equations (1) and (2); K_F and n are both empirical constants.

Van't Hoff thermodynamic fitting equations [26]:

$$lnK = \frac{\Delta ST - \Delta H}{RT} \tag{5}$$

where K is the adsorption equilibrium constant; T is the absolute temperature, K; ΔS is the entropy change, J·$\left(\text{mol·K}^{-1}\right)^{-1}$; and ΔH is the enthalpy change, J·mol^{-1}.

Gibbs free energy change [26]:

$$\Delta G = -\text{R}TlnK \tag{6}$$

where K is the adsorption equilibrium constant; T is the absolute temperature, K; and ΔG is the Gibbs free energy change, kJ·mol^{-1}.

2.5.2. Adsorption Kinetics Fitting

Quasi first-order adsorption kinetic model [27]:

$$ln(Q_e - Q_t) = lnQ_e - k_1 t \tag{7}$$

where Q_t is the adsorption capacity at any time, mg·g^{-1}; Q_e represents the same as in Equation (2); t is the adsorption time, min; and k_1 is the first-order rate constant, h^{-1}.

Quasi-second-order adsorption kinetic model [27]:

$$\frac{t}{Q_e} = \frac{1}{k_2 Q_e^2} + \frac{t}{Q_e} \tag{8}$$

where Q_e represents the same as in Equation (2); t is the adsorption time, min; and k_2 is the second-order rate constant, h^{-1}.

3. Results and Discussion

3.1. XRD and FT-IR Characterization

XRD patterns of composite adsorbents are shown in Figure 1.

As shown in Figure 1, the characteristic peaks of the Zr–La–Fe ternary composite adsorbent were observed at diffraction angles of 31.56°, 45.43°, 56.57°, 67.97°, and 74.95°. Compared with the standard card, the characteristic diffraction peaks of ZrO were located at 31.56° and 67.97°. The characteristic diffraction peaks of La_2O_3 at 45.43° and 74.95° corresponded to the characteristic diffraction peaks of Fe_3O_4 at 56.57°, indicating that the preparation of the ternary composite adsorbent was successful.

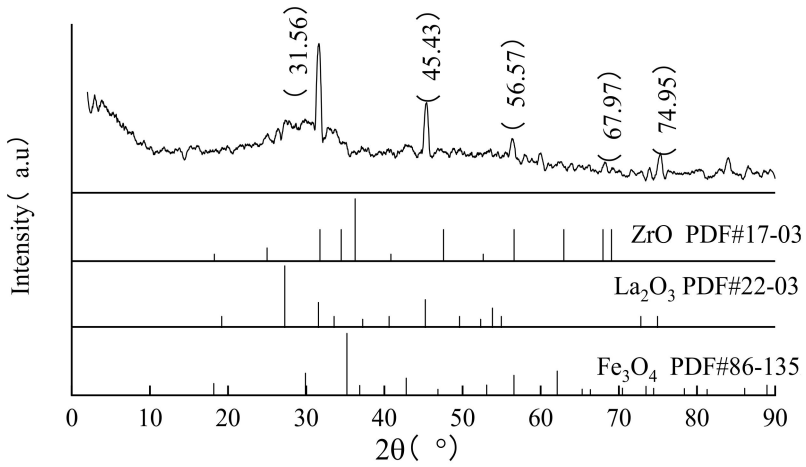

Figure 1. XRD pattern of composite adsorbent and standard card.

3.2. FT-IR Characterization Results and Analysis

The FT-IR spectra of composite adsorbents are shown in Figure 2. As shown in Figure 2, before phosphorus removal, the samples exhibited an O-H deformation vibration peak and C-O stretching vibration peak of sodium alginate at 1400 cm^{-1} and 1090 cm^{-1}, as well as an O-H stretching vibration peak of sodium alginate at 3500 cm^{-1} and H-O-H bending vibration peak of water molecules at 1650 cm^{-1}. After phosphorus removal by adsorption, two new peaks, the P-H stretching vibration peak and P-O stretching vibration peak, were observed at 2350 cm^{-1} and 1080 cm^{-1}, respectively, thus confirming that phosphate had a coordination exchange reaction with surface hydroxyl groups, which enabled phosphorus removal.

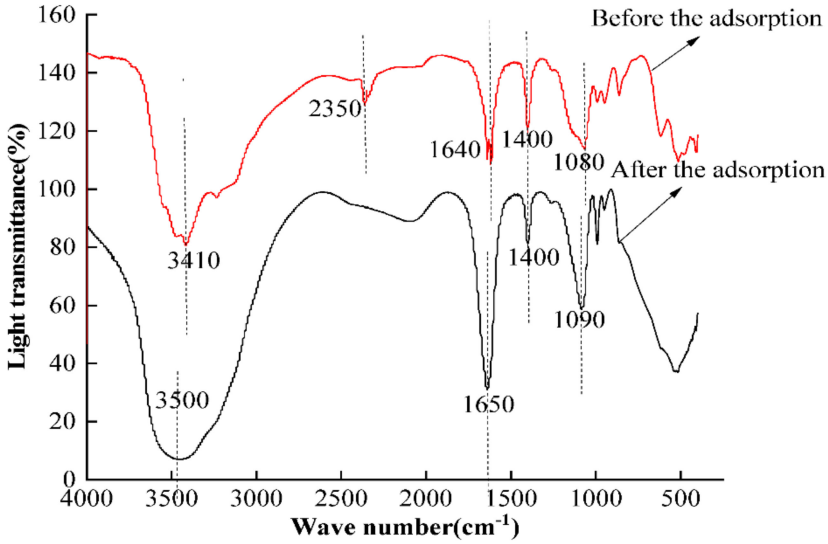

Figure 2. FT–IR spectra of the composite adsorbents before and after adsorption.

3.3. SEM Characterization Results and Analysis

Figure 3 illustrates the SEM images before and after phosphorus adsorption by the composite adsorbent.

As shown in Figure 3, before phosphorus removal by the composite adsorbent, its surface was rough and irregular, and its pore structure was complex. After adsorption and phosphorus removal, some obvious changes occurred in the surface structure, such as a honeycomb structure, increased pore connection, and the formation of granular deposits.

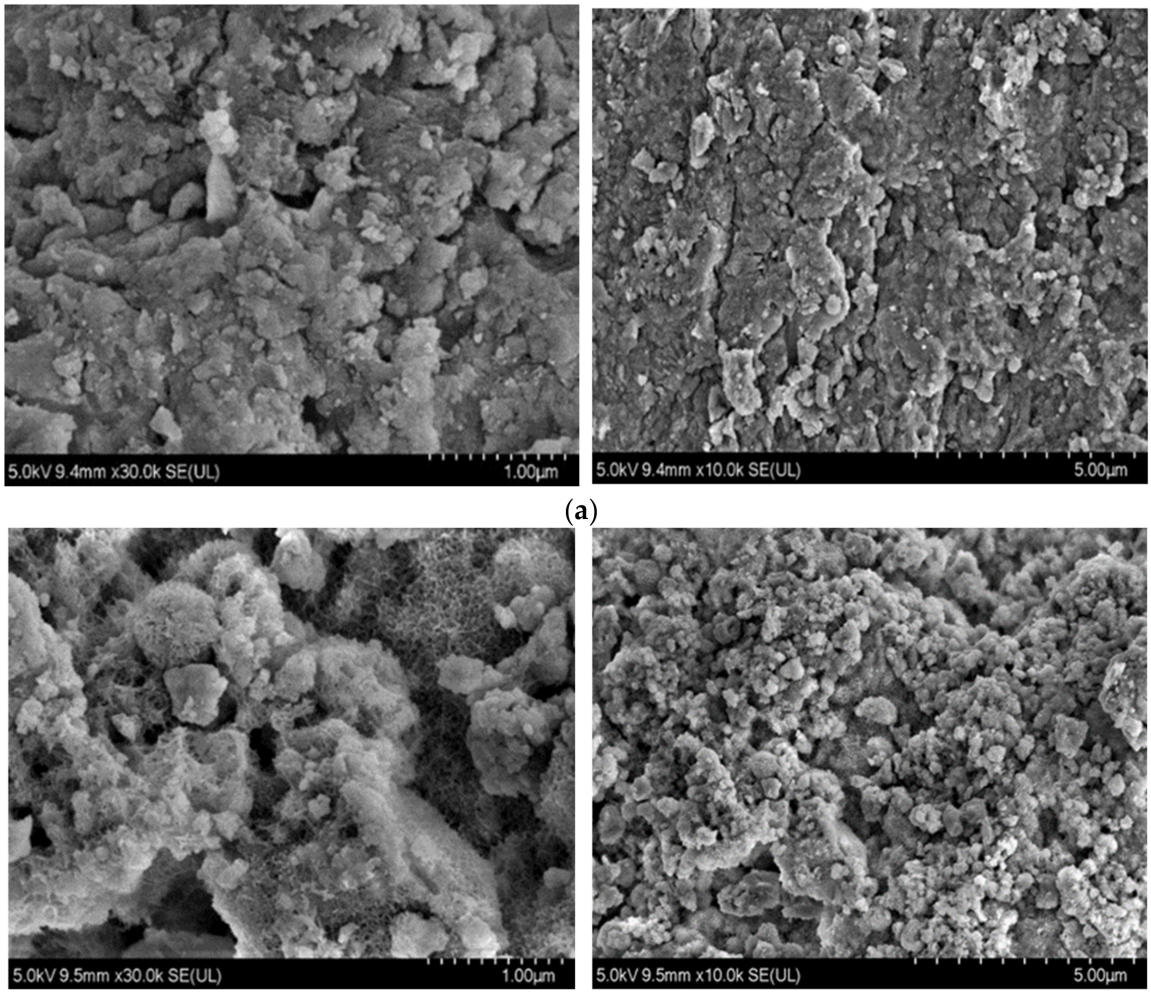

Figure 3. SEM image of composite adsorbents. (**a**) Before adsorption 30,000×; before adsorption 10,000×. (**b**) After adsorption 30,000×; after adsorption 10,000×.

3.4. XPS Characterization Results and Analysis

The full XPS spectrum of the composite adsorbent is shown in Figure 4. As shown in Figure 4, the binding energies of the composite adsorbents correspond to the Zr3d characteristic peaks at 181 eV; the La4d, La3d, and La3p3 characteristic peaks are at 106, 836, and 1129 eV, respectively; and the binding energies of 711 eV correspond to the Fe-OOH characteristic peaks, demonstrating that the preparation of ternary composite adsorbents was successful. The binding energy of 131 eV corresponds to the P2p characteristic peak, confirming the phosphate adsorption reaction.

Figure 5 illustrates the O1s spectrum before and after phosphorus removal by the composite adsorbent. As shown in Figure 5, the proportion of M-OH decreased from 90.10% to 89.11% before and after the adsorption, and the proportion of M-O increased from 9.90% to 10.89%, indicating that hydroxyl M-OH on the metal surface is involved in the removal of phosphorus via adsorption.

3.5. Point-of-Zero-Charge Test

The point of zero charge on the surface of the adsorbed material was determined by potentiometric titration, and the results are shown in Figure 6. A certain mass of composite adsorbent was added into a 0.1 mol·L^{-1} NaCl solution, and the initial pH was adjusted to 5, 7, 9, and 10 with HCl and NaOH. Then, the samples were transferred to a 298 K temperature-controlled shaker for 48 h. The samples were then centrifuged, and the final

pH of the supernatant liquid was determined using a pH meter. Finally, DpH (i.e., the difference between the initial and final pH) was plotted against pH.

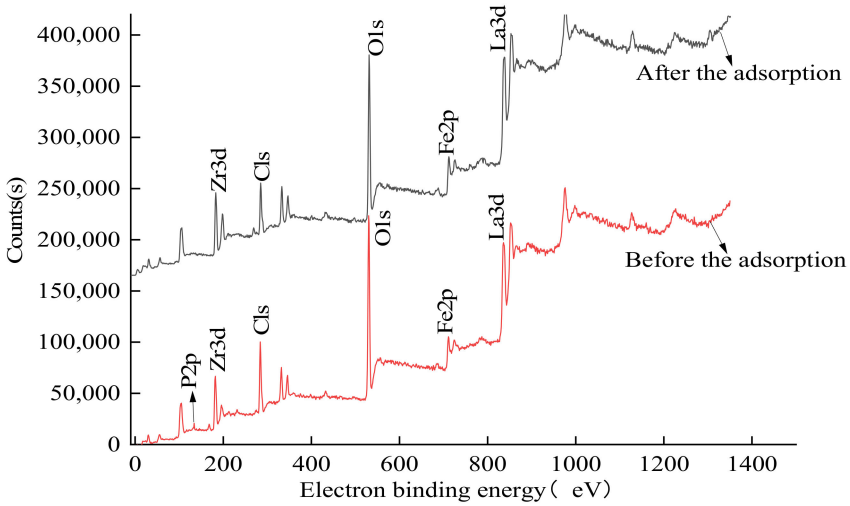

Figure 4. XPS spectra of composite adsorbents.

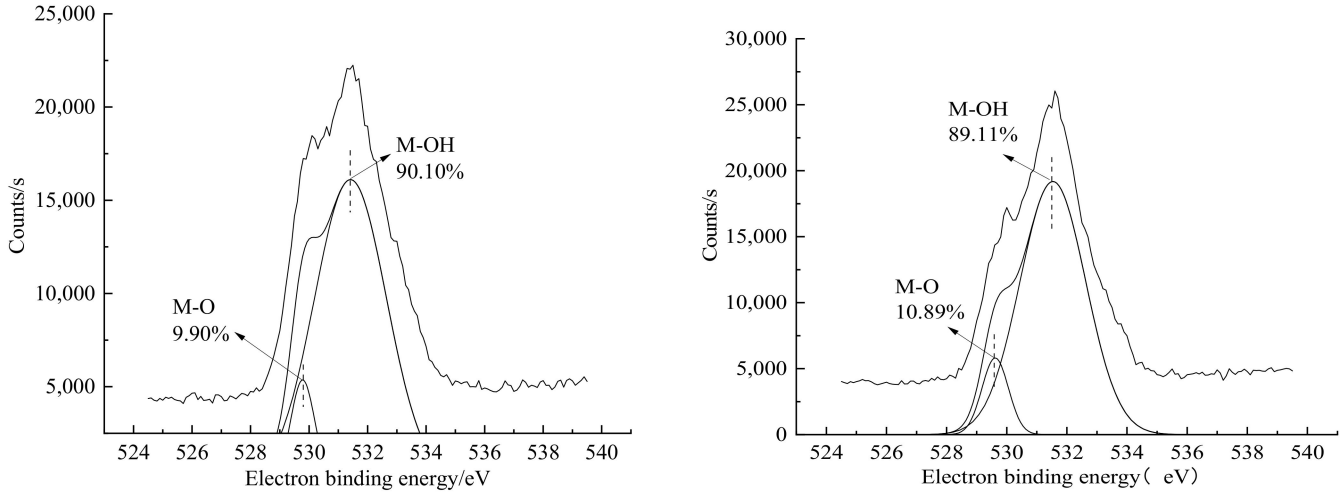

(**a**) (**b**)

Figure 5. XPS spectra of O1s before (**a**) and after (**b**) phosphorus removal by composite adsorbent.

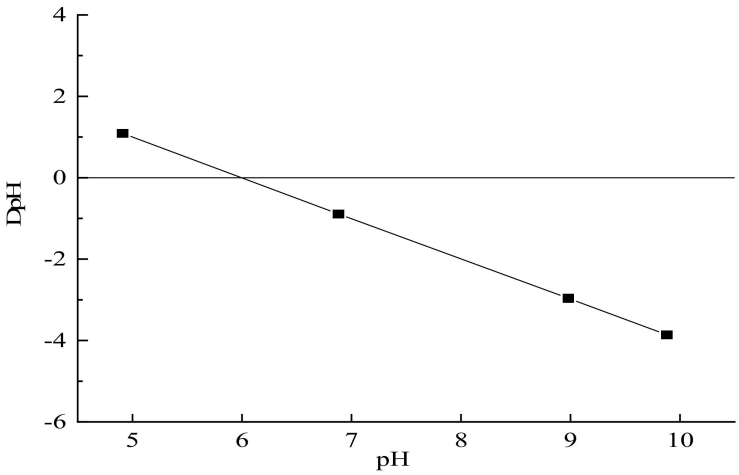

Figure 6. Test chart of surface zero-potential point.

As shown in Figure 6, the point of zero charge of the Zr–La–Fe ternary composite adsorbent embedded with sodium alginate was pH = 6. When pH < 6, the surface of the adsorbent was positively charged due to the proportion of the hydroxyl groups on the surface, which can promote the adsorption of phosphate through electrostatic attraction. When pH > 6, the surface of the adsorbent was electronegative, which was not conducive to the adsorption of phosphate, resulting in a reduced phosphorus removal rate. These results are consistent with the analysis of the influence of pH on phosphorus removal performance in subsequent single-factor experiments.

3.6. Influence of Adsorbent Dosage on Phosphorus Removal Performance

Test conditions: wastewater volume, 50 mL; initial concentration of phosphorus containing wastewater, 10 $mg \cdot L^{-1}$; pH of wastewater, 6; temperature, 25 °C; reaction time, 4 h; shaking speed, 180 $r \cdot min^{-1}$. The test results were obtained by varying the amount of composite adsorbent, as shown in Figure 7.

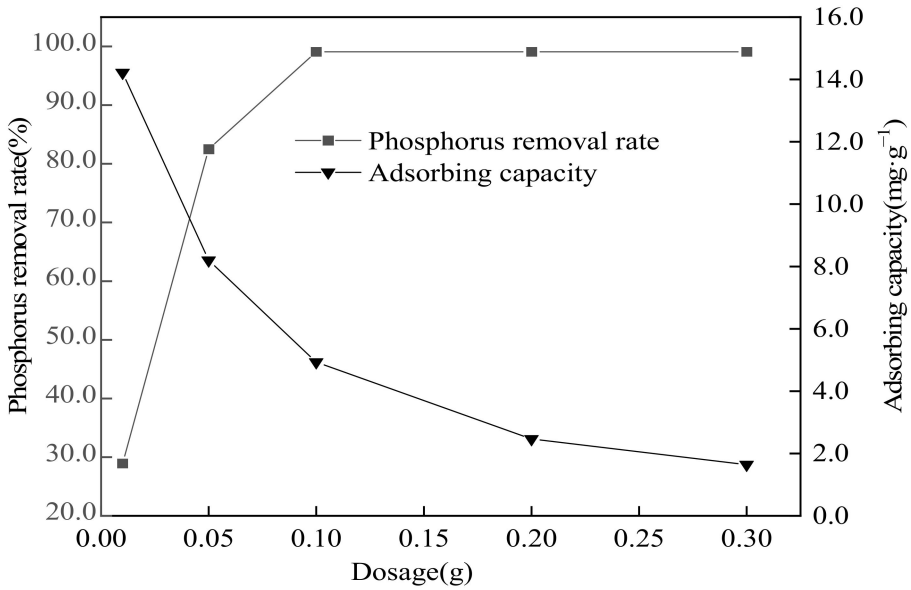

Figure 7. Effect of adsorbent dosage on phosphorus removal performance.

As shown in Figure 7, with the increase in the amount of adsorbent, phosphorus removal first increased rapidly and then gradually stabilized, but the adsorbing capacity decreased slowly. The main reason was that when the initial concentration of phosphorus-containing wastewater is fixed, more active sites are used when the amount of adsorbent increases, thus increasing the removal rate. However, when more adsorbent is added, many active sites are not fully utilized, resulting in a gradual stabilization of the removal rate. The adsorbing capacity is the adsorption quantity of a unit mass of adsorbent when the amount of adsorbate phosphorus is fixed, and increasing the amount of adsorbent is bound to reduce the adsorption capacity. Our findings indicate that the optimal adsorbent dose to meet the "Urban Sewage Treatment Plant Pollutant Discharge Standard" (GB18918-2002) level A standard is 0.1 g.

3.7. Influence of Reaction Time on Phosphorus Removal Performance

Test conditions: all tests were conducted as described in Section 3.6. The adsorption material (0.1 g) was added to the reaction and the other conditions remained unchanged. Test results were obtained by changing the adsorption time, as shown in Figure 8. With increased adsorption time, the phosphorus removal rate of the composite adsorbent increased rapidly and then stabilized. Upon reaching 160 min, the effluent concentration of phosphorus reached the level A standard of the Urban Sewage Treatment Plant Pollutant

Discharge Standard (GB18918-2002). Therefore, the optimal adsorption time was 160 min, and the subsequent single-factor experiment was conducted.

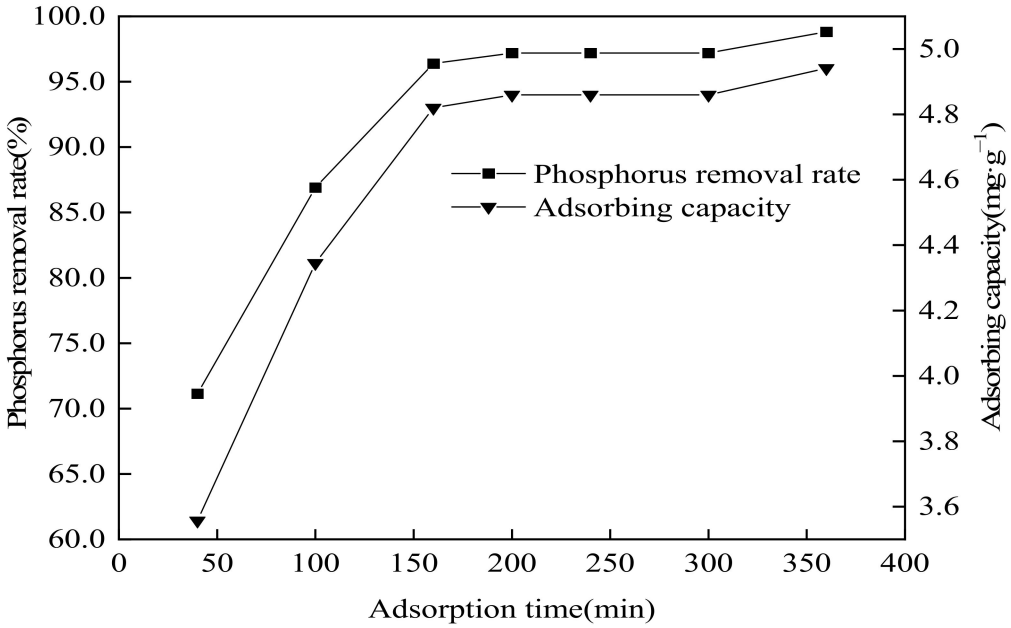

Figure 8. Effect of adsorption time on phosphorus removal performance.

3.8. Influence of pH on Phosphorus Removal Performance of Phosphorus-Containing Wastewater

Test conditions: the test was carried out according to Section 3.7. The reaction time was 160 min, and other conditions remained unchanged. The test results were obtained by changing the pH of wastewater, as shown in Figure 9. The removal rate and adsorption capacity of wastewater decreased when the pH value increased. When the wastewater pH ranged between 4 and 6, the removal rate was above 90%, and the removal rate remained above 80% when the wastewater pH was lower than 7. This change in trend could be explained by the zero-charge point of the material. These findings indicated that the surfaces of the ternary composite adsorbent were protonated and carried positive charges in an acidic medium. However, under alkaline conditions, the surface of the adsorbent is electronegative, and OH^- competes with PO_4^{3-}, thus reducing the removal rate and adsorption capacity of phosphorus. These observations were consistent with those of a previous study [26].

3.9. Influence of Initial Phosphorus Concentration of Wastewater on Phosphorus Removal Performance

Test conditions: All tests were conducted as described in Section 3.8. Other conditions remained unchanged, and the test results were obtained by changing the initial concentration of wastewater, as shown in Figure 10. With the increase in phosphorus concentration in wastewater, the removal rate decreased and the adsorption capacity increased. This is because when the concentration of phosphorus in wastewater is higher, the amount of adsorbent increases when the mass of adsorbent is fixed, and the active sites in wastewater are limited, thus reducing the removal rate. Increasing the adsorbent concentration accelerates its diffusion, as well as phosphorus adsorption capacity.

3.10. Orthogonal Adsorption Experiment

Following an orthogonal experimental design, four factors including time, dosage, initial concentration, and pH were selected, and the results are summarized in Table 1. As shown in Table 1, the optimal phosphorus removal conditions of ternary composite adsorbent embedded with sodium alginate are as follows: initial concentration, 5 mg·L^{-1}; pH, 5; adsorbent dosage, 0.2 g; adsorption time, 200 min. According to the R value range, we concluded that the factors affecting the adsorption effect were the following: dosage of

composite adsorbent > initial concentration of phosphorus-containing wastewater > pH of simulated wastewater > adsorption time.

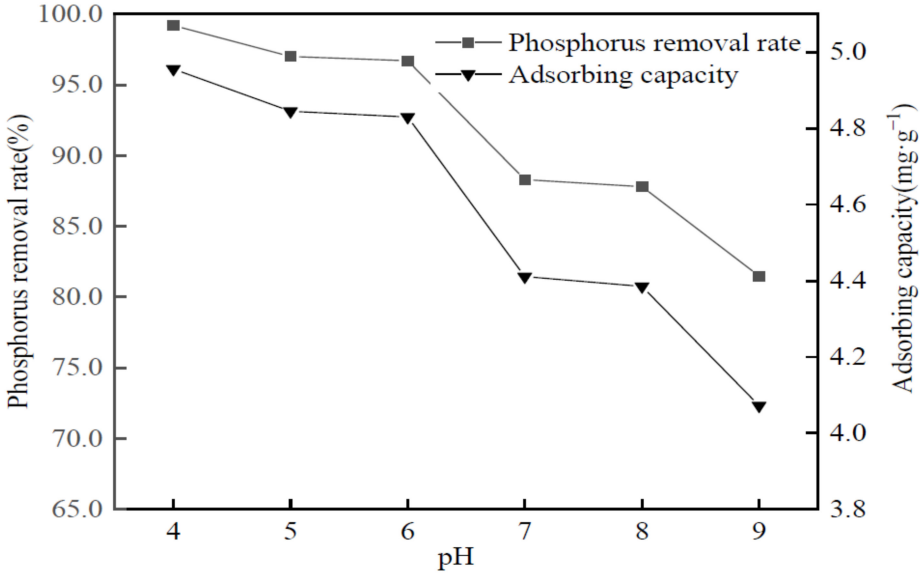

Figure 9. Effect of pH of phosphorus-containing wastewater on phosphorus removal performance.

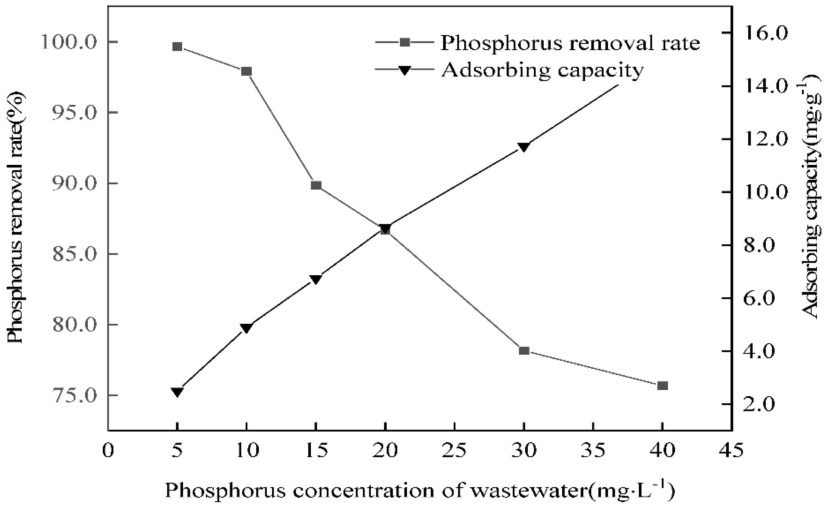

Figure 10. Effect of initial concentration of phosphorus-containing wastewater on phosphorus removal performance.

Under the optimal test conditions, five tests were repeated to verify the repeatability of the results. The results showed that the average phosphorus removal rate of the five tests was 99.88%, and the relative standard deviation was 0.04%. This demonstrated that the experimental results were relatively stable.

3.11. Orthogonal Verification of the Treatment Effect of Composite Adsorbent on Actual Urban Domestic Sewage

Water samples were taken from the inlet of the Yizhou No.1 Sewage Treatment Plant in Hechi City, Guangxi Province, and the optimal process conditions for phosphorus removal were obtained via orthogonal tests to verify the treatment effect of the composite adsorbent prepared in this study on actual domestic sewage. First, the characteristics of the water samples were determined, after which the test conditions were adjusted to conduct three parallel adsorption tests. After the adsorption test, a certain volume of water sample was

removed for digestion and the residual phosphorus concentration was determined by spectrophotometry. Table 2 lists the characteristics of actual urban domestic sewage.

Table 1. Orthogonal experiment results and range analysis.

Test Number	pH	*Initial Concentration* (mg·L^{-1})	*Adsorbent Dosage* (g)	*Adsorption Time* (min)	*Removal Rate* (%)
1	5	5	0.05	100	77.80
2	5	10	0.1	160	86.50
3	5	15	0.2	200	99.60
4	6	5	0.1	200	98.20
5	6	10	0.2	100	98.50
6	6	15	0.05	160	64.13
7	7	5	0.2	160	98.00
8	7	10	0.05	200	68.60
9	7	15	0.1	100	69.67
K_1	263.90	274.00	210.53	245.97	
K_2	260.83	253.60	254.37	248.63	
K_3	236.27	233.40	296.10	266.40	
k_1	87.97	91.33	70.18	81.99	
k_2	86.94	84.53	84.79	82.88	
k_3	78.76	77.80	98.70	88.80	
R	9.21	13.53	28.52	6.81	

Table 2. Characteristics of sewage.

Sewage Quality Parameters	Concentration	Unit
COD	321 ± 0.45	mg·L^{-1}
BOD	180 ± 0.16	mg·L^{-1}
NH_3-N	3.26 ± 0.06	mg·L^{-1}
TP	4.17 ± 0.04	mg·L^{-1}
ORP	365 ± 0.78	mV
pH	6.87 ± 0.05	/
Conductivity	985 ± 0.13	μS/cm

The results showed that the mean concentration of total phosphorus in water samples at the intake of urban sewage treatment plant was 4.17 mg·L^{-1}, and the residual concentration of total phosphorus was not detected after adsorption; that is, the concentration was lower than 0.01 mg·L^{-1}. Therefore, the composite adsorbent prepared in this experiment had a significant effect on the treatment of low-concentration municipal wastewater, and could reduce the concentration of total phosphorus in municipal wastewater treatment plant influents to close to 0 mg·L^{-1}. These characteristics highlight the applicability of the adsorbent.

3.12. Results of Adsorption Isotherm Fitting

Experimental conditions: the volume of wastewater was 50 mL; the amount of adsorbent was 0.1 g; the initial concentrations of phosphorus-containing wastewater were 5, 10, 15, 20, 30, and 40 mg·L^{-1}; pH was 6; the experiments were conducted at three temperatures (25 °C, 40 °C and 55 °C); and the shock adsorption was 160 min. The isotherm fitting results are shown in Figure 11 and Table 3.

As shown in Table 3, under three different temperature conditions, the linear correlation coefficient of the Freundlich model was higher, indicating that the reaction process was more consistent with the Freundlich adsorption isotherm equation. The adsorption index 1/n was between 0.1 and 0.5, indicating that phosphorus was readily removed via adsorption.

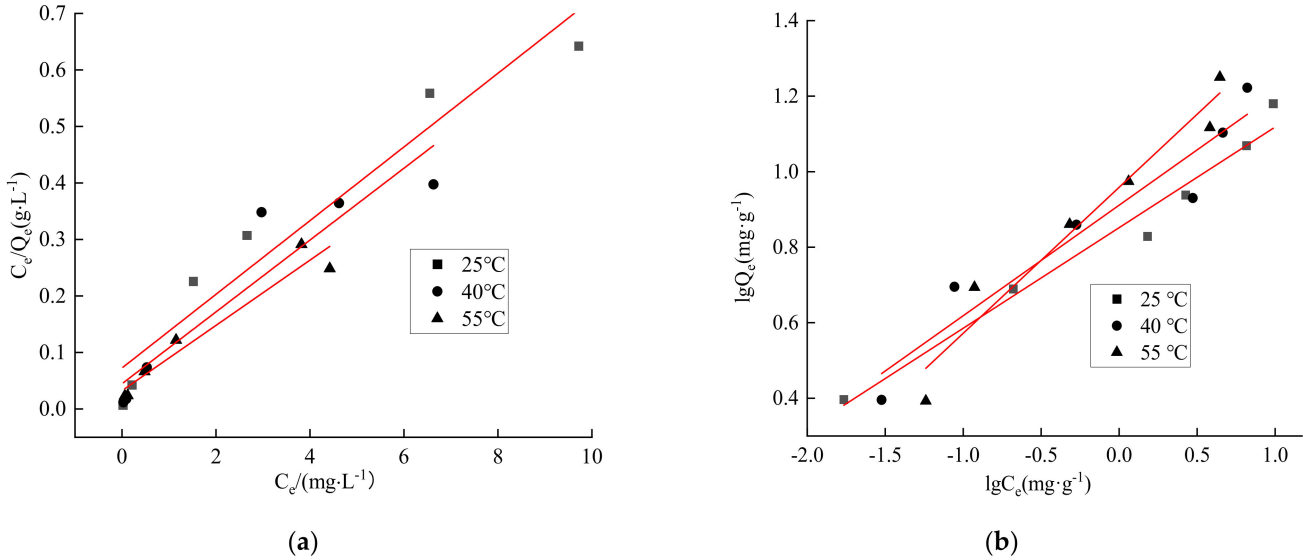

(**a**) (**b**)

Figure 11. Langmuir (**a**) and Freundlich adsorption isotherm (**b**).

Table 3. Fitting results of two isothermal lines.

	Langmuir Model			Freundlich Model		
Temperature (°C)	**a**	**Q_m/(mg·g^{-1})**	**R^2**	**k**	**1/n**	**R^2**
25	0.07	15.3	0.9394	7.11	0.27	0.9729
40	0.04	15.7	0.8792	8.15	0.29	0.9234
55	0.03	17.3	0.9406	9.02	0.39	0.9513

According to the adsorption isotherm data, the calculation results are shown in Figure 12 and Table 4.

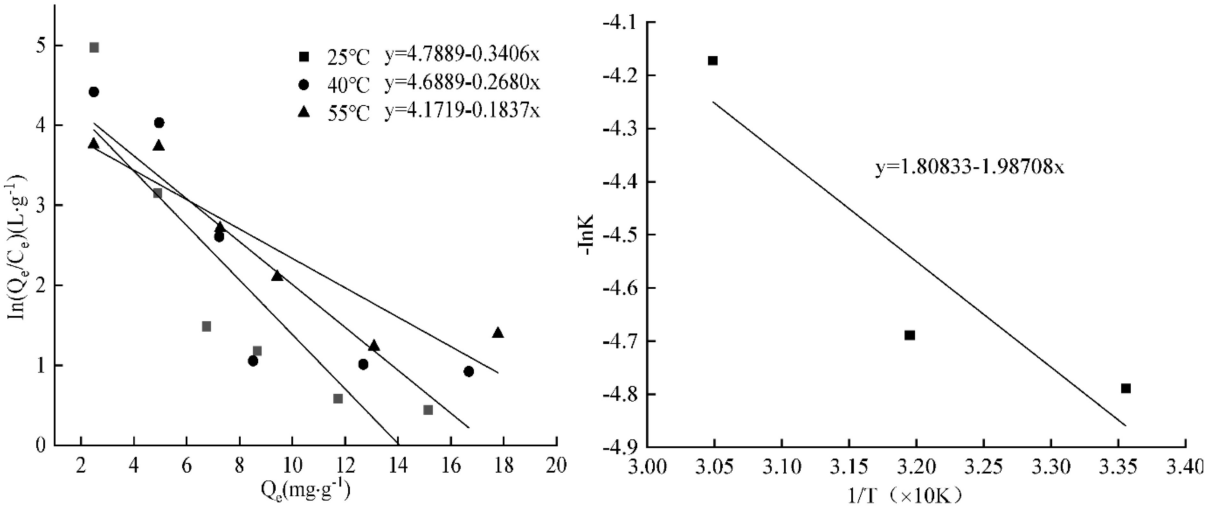

Figure 12. Thermodynamic calculation fitting of adsorption.

Table 4. Thermodynamic constants of phosphorus adsorption on composite adsorbents at different temperatures.

Thermodynamic Constant	298 K	313 K	328 K
ΔG/(kJ·mol^{-1})	−11.9	−12.2	−11.4
ΔH/(kJ·mol^{-1})	−16.5	−16.5	−16.5
ΔS/(J·mol^{-1}·K^{-1})	15.0	15.0	15.0

As shown in Table 4, the ΔG values of the three Gibbs free energy variations at different temperatures were all negative, indicating that the adsorption reaction could occur spontaneously. The ΔH enthalpy changes were all negative, indicating that the reaction was exothermic. The ΔS entropy changes were all positive, indicating that adsorption can increase the confusion degree of the solid–liquid interface, and also demonstrating that adsorption can occur spontaneously.

3.13. Results of Adsorption Kinetics Fitting

The fitting results of adsorption kinetics are shown in Figure 13 and Table 5. It can be seen from Table 5 that the adsorption process is more consistent with the quasi-second-order kinetic equation by comparing the linear correlation coefficients. The results demonstrate that the adsorption process is based on the compound effect of multiple adsorption mechanisms, meaning that the adsorption rate is affected by multiple factors such as wastewater pH, concentration, and electron sharing or electron transfer between adsorbent and adsorbate. The chemisorption is the primary controlling step because that is the basic assumption of the quasi-second-order kinetic model.

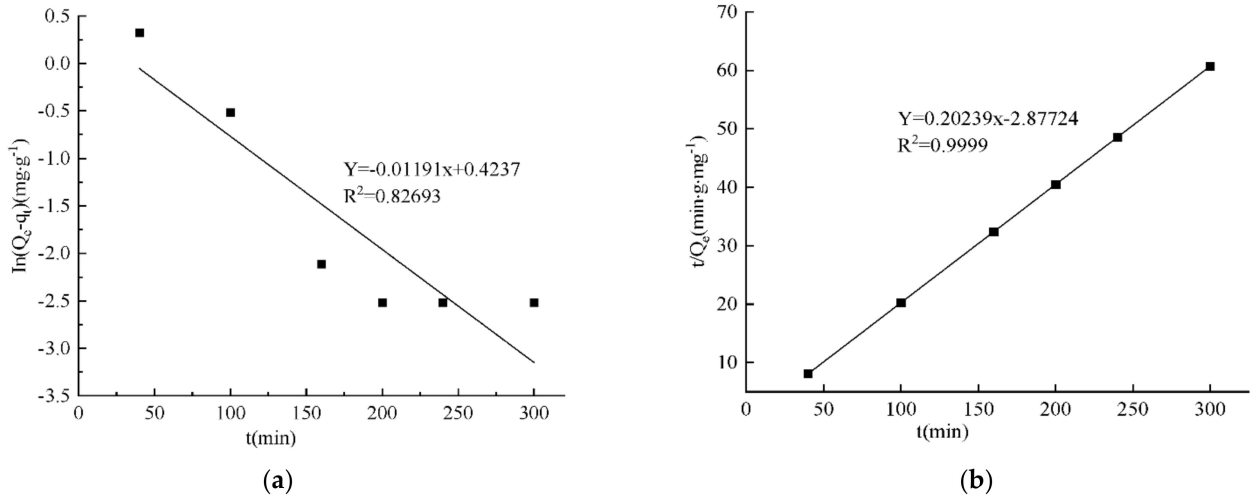

(**a**) (**b**)

Figure 13. Quasi-first-order kinetic model (**a**) and quasi-second-order kinetic model (**b**).

Table 5. Quasi-first-order and quasi-second-order adsorption kinetics fitting parameters.

Quasi First Order Dynamics Model			Quasi Second Order Dynamics Model		
Q_e/(mg·g^{-1})	k_1/h^{-1}	R^2	Q_e/(mg·g^{-1})	k_2/h^{-1}	R^2
1.53	0.0119	0.8269	4.94	0.0142	0.9999

3.14. Regeneration Performance of Composite Adsorbent

The first adsorption test was carried out under optimal adsorption conditions, after which the adsorbed samples were centrifuged and dried in a drying oven at 50 °C. After cooling, a 0.5 mol·L^{-1} sodium hydroxide solution was used for desorption for 3 h. The samples were then centrifuged, and the desorption materials were recovered after drying in a drying oven at 50 °C. The recovered material was then used for a second adsorption, and the adsorption–desorption cycle was repeated three times. Through this test, the regeneration capacity of the adsorbed material was determined, and the test results are shown in Figure 14.

As illustrated in Figure 14, after two regeneration cycles, the removal rate of 5 mg·L^{-1} phosphorous wastewater by the embedded composite adsorbent decreased to 83.53%. After three cycles of desorption and adsorption, the removal rate of phosphorus by the adsorbent remained above 68%, indicating that the embedded composite adsorbent prepared in this

experiment could be effectively used up to three times, after which its absorbance capacity decreased significantly.

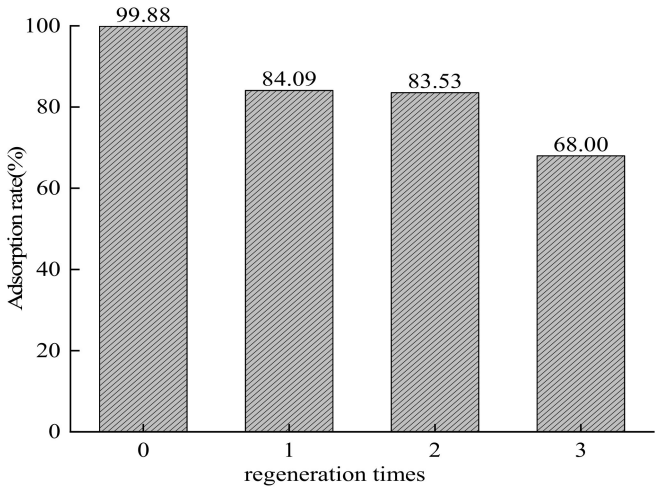

Figure 14. Effect of continuous regeneration cycles on the adsorption rates of the adsorbent.

4. Conclusions

The mechanism of phosphorus removal by the sodium alginate-embedded Zr–La–Fe ternary composite adsorbent prepared in this experiment is mainly based on the coordination of phosphate at the metal active site and the coordination exchange reaction with the surface hydroxyl groups, resulting in granular phosphate deposits. The prepared adsorbent not only exhibited a high adsorption performance on laboratory-simulated wastewater, but was also effective on actual domestic wastewater, thus providing a promising new approach for the treatment of phosphorus-containing wastewater. The adsorption process was more consistent with the Freundlich adsorption isotherm equation and quasi-second-order kinetic model, and the adsorption phosphorus removal reaction was exothermic and could be spontaneous. After three lye regeneration tests, the removal rate of phosphorus in water remained above 68%, and the granulation of the adsorbent was achieved via embedding immobilization technology, which overcomes the problem of the easy loss of powder adsorbent, thus enabling the recycling of the adsorbent.

Author Contributions: Data collation and analysis, writing—original draft, X.L.; adsorption single-factor and orthogonal experiment, H.L.; characterization of materials and regeneration performance of adsorbent, Y.M.; funding acquisition, project administration, supervision, writing—review and editing, Y.W.; All authors have read and agreed to the published version of the manuscript.

Funding: This work was financially supported by the 2021 Young and Middle-aged Teachers' Scientific Research Basic Ability Promotion Project of Guangxi University (No. 2021KY0616), as well as the 2022 Autonomous Region-level College Students' Innovation and Entrepreneurship Training Plan (No. S202210605052).

Institutional Review Board Statement: Not applicable.

Informed Consent Statement: Not applicable.

Data Availability Statement: Not applicable.

Acknowledgments: The authors would like to thank all the reviewers who participated in the review.

Conflicts of Interest: The authors declare no conflict of interest.

References

1. Kim, J.-O.; Chung, J. Implementing chemical precipitation as a pretreatment for phosphorus removal in membrane bioreactor-based municipal wastewater treatment plants. *KSCE J. Civ. Eng.* **2014**, *18*, 956–963. [CrossRef]
2. Wang, H.; Tian, Z.; Wang, H.; Yan, Q. Optimization and reaction kinetics analysis for phosphorus removal in struvite precipitation process. *Water Environ. Res.* **2020**, *92*, 1162–1172. [CrossRef] [PubMed]

3. Ochoa, C.; Hernández, M.A.; Bayona, O.L.; Camargo, H.A.; Cabeza, I.O.; Candela, A.M. Phosphorus recovery by struvite from anaerobic co-digestion effluents during residual biomass treatment. *Biomass Convers. Biorefin.* **2020**, *11*, 261–274. [CrossRef]
4. Izadi, P.; Eldyasti, A. Design, operation and technology configurations for enhanced biological phosphorus removal (EBPR) process: A review. *Rev. Environ. Sci. Bio/Technol.* **2020**, *19*, 561–593. [CrossRef]
5. Matsuura, N.; Masakke, Y.; Karthikeyan, S.; Kanazawa, S.; Honda, R.; Yamamoto-Ikemoto, R.; Konstantinidis, K.T. Metagenomic insights into the effect of sulfate on enhanced biological phosphorus removal. *Appl. Microbiol. Biotechnol.* **2021**, *105*, 2181–2193. [CrossRef]
6. Banu, J.R.; Merrylin, J.; Kavitha, S.; Kannah, R.Y.; Selvakumar, P.; Gopikumar, S.; Sivashanmugam, P.; Do, K.-U.; Kumar, G. Trends in Biological Nutrient Removal for the Treatment of Low Strength Organic Wastewaters. *Curr. Pollut. Rep.* **2021**, *7*, 1–30. [CrossRef]
7. Khalil, A.K.A.; Dweiri, F.; Almanassra, I.W.; Chatla, A.; Atieh, M.A. Mg-Al Layered Double Hydroxide Doped Activated Carbon Composites for Phosphate Removal from Synthetic Water: Adsorption and Thermodynamics Studies. *Sustainability* **2022**, *14*, 6991. [CrossRef]
8. Huang, C.; Tang, C.; Wu, Q.; Zhu, Q. Magnetic $MnFe_2O_4$/ZnFe-LDH for Enhanced Phosphate and Cr (VI) Removal from Water. *Environ. Sci. Pollut. Res.* **2022**, *29*, 59224–59234. [CrossRef]
9. Feng, L.; Zhang, Q.; Ji, F.; Jiang, L.; Liu, C.; Shen, Q.; Liu, Q. Phosphate removal performances of layered double hydroxides (LDH) embedded polyvinyl alcohol/lanthanum alginate hydrogels. *Chem. Eng. J.* **2021**, *430*, 132754. [CrossRef]
10. Alagha, O.; Manzar, M.S.; Zubair, M.; Anil, I.; Mu'Azu, N.D.; Qureshi, A. Comparative Adsorptive Removal of Phosphate and Nitrate from Wastewater Using Biochar-MgAl LDH Nanocomposites: Coexisting Anions Effect and Mechanistic Studies. *Nanomaterials* **2020**, *10*, 336. [CrossRef]
11. Parasana, N.; Shah, M.; Unnarkat, A. Recent advances in developing innovative sorbents for phosphorus removal—Perspective and opportunities. *Environ. Sci. Pollut. Res.* **2022**, *29*, 38985–39016. [CrossRef]
12. Xu, Z.; Zhong, Y.; Wang, Y.; Song, X.; Huang, W. Removal performance and mechanism of phosphorus by different Fe-based layered double hydroxides. *Environ. Sci. Pollut. Res.* **2022**, 1–11. [CrossRef]
13. Yuan, J.; Zhu, Y.; Wang, J.; Liu, Z.; He, M.; Zhang, T.; Li, P.; Qiu, F. Facile Modification of Biochar Derived from Agricultural Straw Waste with Effective Adsorption and Removal of Phosphorus from Domestic Sewage. *J. Inorg. Organomet. Polym. Mater.* **2021**, *31*, 3867–3879. [CrossRef]
14. Duan, H.; Zhang, L.; Wang, Y.; Liu, Y.; Wang, Y. Phosphate removal from aqueous solution by Fe–La binary (hydr)oxides: Characterizations and mechanisms. *Environ. Sci. Pollut. Res.* **2021**, *28*, 62662–62676. [CrossRef]
15. Zhang, X.; Ma, C.; Wen, K.; Han, R. Adsorption of phosphate from aqueous solution by lanthanum modified macroporous chelating resin. *Korean J. Chem. Eng.* **2020**, *37*, 766–775. [CrossRef]
16. Park, Y.; Gorman, C.; Ford, E. Lanthanum carbonate nanofibers for phosphorus removal from water. *J. Mater. Sci.* **2020**, *55*, 5008–5020. [CrossRef]
17. Nakarmi, A.; Moreira, R.; Bourdo, S.E.; Watanabe, F.; Toland, A.; Viswanathan, T. Removal and Recovery of Phosphorus from Contaminated Water Using Novel, Reusable, Renewable Resource-Based Aluminum/Cerium Oxide Nanocomposite. *Water Air Soil Pollut.* **2020**, *231*, 559. [CrossRef]
18. Qiu, L.; Zhang, M.; Yu, X.; Zheng, P. A novel Fe(II)-Ca synergistic phosphorus removal process: Process optimization and phosphorus recovery. *Environ. Sci. Pollut. Res.* **2017**, *25*, 1543–1550. [CrossRef]
19. Banu, R.J.; Do, K.U.; Yeom, I.T. Phosphorus removal in low alkalinity secondary effluent using alum. *Int. J. Environ. Sci. Technol.* **2007**, *5*, 93–98. [CrossRef]
20. Liu, B.; Lou, S.; Zeng, Y.; Qin, Y.; Zhang, W.; Zhang, L.; Liu, X. High-efficiency adsorption of phosphate by Fe-Zr-La tri-metal oxide composite from aqueous media: Performance and mechanism. *Adv. Powder Technol.* **2021**, *32*, 4587–4598. [CrossRef]
21. Yu, Y.; Chen, J.P. Key factors for optimum performance in phosphate removal from contaminated water by a Fe–Mg–La tri-metal composite sorbent. *J. Colloid Interface Sci.* **2015**, *445*, 303–311. [CrossRef] [PubMed]
22. Yu, Y.; Yu, L.; Chen, J.P. Adsorption of fluoride by Fe–Mg–La triple-metal composite: Adsorbent preparation, illustration of performance and study of mechanisms. *Chem. Eng. J.* **2015**, *262*, 839–846. [CrossRef]
23. Lu, J.; Liu, H.; Liu, R.; Zhao, X.; Sun, L.; Qu, J. Adsorptive removal of phosphate by a nanostructured Fe–Al–Mn trimetal oxide adsorbent. *Powder Technol.* **2013**, *233*, 146–154. [CrossRef]
24. Langmuir, I. The constitution and fundamental properties of solids and liquids. *J. Am. Chem. Soc.* **1916**, *38*, 2221–2295. [CrossRef]
25. Freundlich, H. Uber die adsorption in lasungen. *J. Z. Phys. Chem.* **1906**, *57*, 385–470. [CrossRef]
26. Yang, H.; Luo, B.; Zhang, Y.; Zhou, B.; Ahmed, S.M.; Liu, H.; Liu, X.; He, Y.; Xia, S. Study of Humic Acid Adsorption Character on Natural Maifan Stone: Characterization, Kinetics, Adsorption Isotherm, and Thermodynamics. *ACS Omega* **2020**, *5*, 7683–7692. [CrossRef]
27. Zubair, M.; Manzar, M.S.; Suleiman, M.A.; Fernandes, D.P.; Meili, L.; Al Bin Essa, W.; Al-Adam, H.; AlGhamdi, J.M.; Mu'Azu, N.D.; Haladu, S.A.; et al. Production of magnetic biochar-steel dust composites for enhanced phosphate adsorption. *J. Water Process Eng.* **2022**, *47*, 102793. [CrossRef]